

Precessional modes due to spin-transfer in spin-valve nanopillars

M. GMITRA^{1,3*}, J. BARNAŚ², D. HORVÁTH³

¹Department of Physics, Adam Mickiewicz University, UL. Umultowska 85, 61-614 Poznań, Poland

²Institute of Molecular Physics, Polish Academy of Sciences,
M. Smoluchowskiego 17, 60-179 Poznań, Poland

³Department of Theoretical Physics and Astrophysics, P. J. Šafárik University,
Park Angelinum 9, 040 01 Košice, Slovak Republic

Current-driven magnetic switching and magnetic dynamics in spin-valve nanopillars are considered in the framework of the macrospin model. The corresponding spin transfer torque is calculated in terms of the macroscopic model based on spin diffusion equations. Critical currents for switching from parallel to antiparallel magnetic configurations and to precessional regime are derived. Frequencies of the precessional modes are also calculated as a function of external magnetic field and electric current.

Key words: *spin-transfer; switching; spintronics*

1. Introduction

The quantum-mechanical phenomenon of spin transfer between polarized conduction electrons and localized magnetic moments of a thin magnetic film can induce switching and/or precession of the film magnetization [1]. The current-driven magnetization manipulation has been observed in experiments carried out on multilayers, nanowires, small particles, tunnel junctions, and nanopillar spin valves. The latter ones provide the most convincing experimental data [2, 3]. A typical nanopillar spin valve consists of thick and thin magnetic layers separated by a non-magnetic spacer layer, the thick layer acting as a source of spin current. Several theoretical models have also been developed to describe physical mechanisms of the spin-transfer and magnetic switching phenomena [4–7].

*Corresponding author, e-mail: martin.gmitra@upjs.sk

It has also been found that at some conditions electric current can cause transition to steady precessional modes where the energy is pumped from conduction electrons to localized magnetic moments [8, 9]. This phenomenon is of high importance due to possible applications in microwave generation. In typical Co/Cu/Co spin-valve systems, the precessional modes were found in a non-zero external magnetic field and for current exceeding certain critical value [10–13]. The critical current depends on the applied external magnetic field and intrinsic parameters of the nanopillar, like interfacial resistances, bulk resistivities, demagnetization field, anisotropy field or damping parameter of a thin film. In Co/Cu/Co spin valves, the current-induced steady precessions exist for external magnetic fields larger than the anisotropy field of the thin layer [10, 11]. For lower values of external field, the current drives switching to anti-parallel (AP) or parallel (P) states, depending on the initial state of the system [12].

In this paper, we present the effects of spin-transfer torque on steady magnetization precessions, whose frequency can be manipulated by the external magnetic field and current density flowing through the system. We also discuss current-driven transition between two kinds of steady precessions.

2. Macrospin model

We consider a tri-layer system which is attached to two external nonmagnetic leads. A qualitative behaviour of a thin (free or sensing) layer can be described within the single-domain approximation (macrospin model) [10, 13]. Magnetic dynamics of the sensing layer is then described by the generalized Landau–Lifshitz–Gilbert equation:

$$\frac{d\hat{\mathbf{s}}}{dt} = -|\gamma_g| \mu_0 \hat{\mathbf{s}} \times \mathbf{H}_{\text{eff}} - \alpha \hat{\mathbf{s}} \frac{d\hat{\mathbf{s}}}{dt} + \frac{|\gamma_g|}{M_s d} \boldsymbol{\tau} \quad (1)$$

where $\hat{\mathbf{s}}$ is the unit vector along the spin moment of the sensing layer, γ_g is the gyromagnetic ratio, μ_0 is the magnetic vacuum permeability, \mathbf{H}_{eff} is an effective magnetic field acting on the sensing layer, α is the damping parameter, M_s stands for the saturation magnetization, and d is the layer thickness. The effective field includes an external magnetic field H_{ext} , the uniaxial magnetic anisotropy field H_a , and the anisotropy due to the demagnetization field H_d :

$$\mathbf{H}_{\text{eff}} = -H_{\text{ext}} \hat{\mathbf{e}}_z - H_a (\hat{\mathbf{s}} \cdot \hat{\mathbf{e}}_z) \hat{\mathbf{e}}_z + H_d (\hat{\mathbf{s}} \cdot \hat{\mathbf{e}}_x) \hat{\mathbf{e}}_x$$

where $\hat{\mathbf{e}}_x$ and $\hat{\mathbf{e}}_z$ are the unit vectors along the axes x (normal to the layers) and z (in-plane), respectively. The last term in Eq. (1) stands for the torque due to spin transfer,

$$\boldsymbol{\tau} = a I \hat{\mathbf{s}} \times (\hat{\mathbf{s}} \times \hat{\mathbf{S}}) + b I \hat{\mathbf{s}} \times \hat{\mathbf{S}}$$

Here, $\hat{\mathbf{S}}$ is the unit vector along the spin moment of the thick (fixed) magnetic layer ($\hat{\mathbf{S}} = \hat{\mathbf{e}}_z$), a and b are the parameters that generally depend on the intrinsic nanopillar parameters and on magnetic configuration of the system [7]. The current I is defined as positive when it flows from the thick magnetic layer towards the thin one. On linearizing Eq. (1) and performing standard stability analysis, one finds the critical current that destabilizes the P ($\hat{\mathbf{s}} = \hat{\mathbf{S}}$) configuration in the form [14]

$$I_c = \frac{\alpha\mu_0 M_s d}{a - b\alpha} \left(H_a + H_{\text{ext}} + \frac{H_d}{2} \right) \quad (2)$$

where the parameters a and b are to be calculated for the P configuration. For $I > I_c$, the system is driven to AP state for $H_{\text{ext}} < H_a$ and to steady precessional regime for $H_{\text{ext}} > H_a$ [10, 15].

3. Numerical results

The numerical analysis is focused on the current-driven oscillatory magnetoresistance behaviour of the nanopillar Cu/Co(30)/Cu(10)/Co(4)/Cu (the numbers are layer thicknesses in nanometers). For the sensing layer, we assume saturation magnetization $M_s = 17.8$ kOe, anisotropy field $H_a = 986$ Oe, demagnetization field $H_d = 0.65M_s$, and the Gilbert damping parameter $\alpha = 0.003$. The current induced torque, actually the parameters a and b , have been calculated in terms of a macroscopic model in the diffusive transport regime [7], assuming that the spin current component perpendicular to the spin moment of the sensing layer is entirely absorbed in the interfacial region [4, 5]. The calculations have been performed for typical parameters obtained from CPP GMR experiments [16]. For the Co layers we assumed the bulk resistivity $\rho^* = 5.1 \mu\Omega\cdot\text{cm}$, spin asymmetry factor $\beta = 0.51$, and spin-flip length $l_{sf} = 60$ nm, and for Cu layers $\rho^* = 0.5 \mu\Omega\cdot\text{cm}$, $l_{sf} = 1000$ nm. In turn, for Co/Cu interfaces we assume the interfacial resistance $R^* = 0.52 \times 10^{-15} \Omega\cdot\text{m}^2$, the interface spin asymmetry factor $\gamma = 0.76$, and the mixing conductances $\text{Re}\{G_{\uparrow\downarrow}\} = 0.542 \times 10^{15} \Omega^{-1}\cdot\text{m}^{-2}$ and $\text{Im}\{G_{\uparrow\downarrow}\} = 0.016 \times 10^{15} \Omega^{-1}\cdot\text{m}^{-2}$.

The simulations were started with a nearly P configuration and for $I > I_c$ (the initial in-plane spin bias shift of the order of one degree was assumed). The inset in Fig. 1a shows the current dependence of the switching time t_0 from the P configuration to steady precessional regime for the magnetic fields as indicated. The switching time t_0 is defined as the point where $\hat{\mathbf{s}}$ crosses zero for the first time. The current dependence of t_0 reveals a simple rational behaviour. However, the slope of the inverse plot does not depend on the applied magnetic field but we found its significant dependence on the initial bias (not shown). From the latter it follows that duration of the transient regime can be significantly affected by the initial bias, dependent, for example, on the thermal noise.

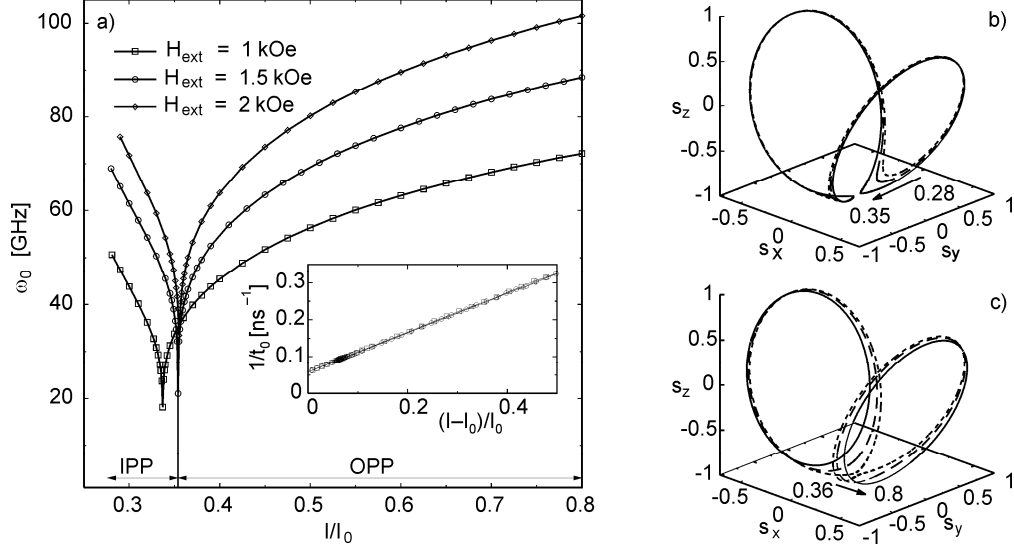


Fig. 1. Fundamental frequency of the magnetoresistance oscillations in Cu/Co(30)/Cu(10)/Co(4)/Cu (a), calculated as a function of the reduced current density, where $I_0 = 10^8$ A/cm², and for magnetic fields as indicated. The inset shows the corresponding current dependence of the switching times (see text) for $H_{\text{ext}} = 1.5$ kOe; steady in-plane orbits for $I/I_0 = 0.28, 0.3, 0.35$ (b), and out-of-plane orbits for $I/I_0 = 0.36, 0.50, 0.80$ for $H_{\text{ext}} = 1.5$ kOe (c). The arrows indicate the change in orbits as the current increases

The fundamental frequency ω_0 (first harmonics) of the magnetoresistance oscillations is shown in Fig. 1a as a function of the current density and for different magnetic fields. The frequency first decreases with increasing current, and then increases showing a profound minimum. To understand the current dependence of the frequency, it is instructive to analyze steady spin orbits of the sensing layer. Figure 1b shows saddle-shaped in-plane precession (IPP) orbits. The arrow indicates the change in orbits as the current increases. Along the segments where \hat{s} moves almost in the layer plane, the spin precesses mainly around H_a and H_{ext} , with the angular velocity proportional to $|\gamma_g|(H_a + H_{\text{ext}})$. Along the remaining part (\hat{s} moves almost perpendicularly to the layer plane), the angular velocity is higher and proportional to $|\gamma_g|(H_a + H_{\text{ext}} + H_d)$. With increasing I , the average orbital speed decreases while the arc length of the orbit increases. Consequently, ω_0 decreases with increasing I .

At a certain value of the current, at which the segments touch each other near the $-z$ axis, the IPP orbit bifurcates into two so-called out-of-plane (OOP) orbits (Fig. 1c). The orbits are interchangeable with respect to the $x \rightarrow -x$ and $y \rightarrow -y$ reflections. The mirror symmetry with respect to the x axis has been reported in Ref. [13]. In our case, the additional mirror symmetry with respect to the y axis is due to a non-zero value of b . A further increase in current increases spin torque and tends to push the orbit away from the layer plane. The arc length decreases and orbital speed increases due to larger demagnetization field. Consequently, ω_0 increases with increasing I .

The frequency ω_0 increases with the increased external magnetic field in both, IPP and OPP cases. We compared the field dependence of the recorded ω_0 for selected current densities to the Kittel formula for small-angle elliptical precession of a thin film ferromagnet. For OPP we have found an increase in effective demagnetization term with increased current. Although, the formula fits very well to the $\omega_0(H_{\text{ext}})$ dependence, the effective demagnetization term differs from that considered in simulation. Similar discrepancies have been observed in experiments [10, 11]. The discrepancy can be associated with an additional effective field induced due to spin-transfer which pumps energy to the system and enables such precessions. In turn, for IPP the $\omega_0(H_{\text{ext}})$ reveals a dependence that cannot be fitted to the Kittel formula.

4. Conclusions

Spin polarized current is shown to drive magnetic switching and steady oscillations of the magnetic moment of the sensing layer. Frequency of the oscillations has been calculated as a function of the magnetic field and electric current. Two kinds of steady orbits have been revealed: in-plane and out-of-plane. The main features of these steady precessions have been also discussed.

Acknowledgements

This work has been partly supported by the Slovak Ministry of Education as a research project MVTs POL/SR/UPJS07, Slovak Grant Agency VEGA 1/2009/05, and by EU through RTN Spintronics (contract HPRN-CT-2000-000302).

References

- [1] SLONCZEWSKI J.C., J. Magn. Magn. Mater., 159 (1996), L1; 195 (1999), L261; BERGER L., Phys. Rev. B, 54 (1996), 9353.
- [2] KATINE J.A., ALBERT F.J., BUHRMAN R.A., MYERS E.B., RALPH D.C., Phys. Rev. Lett., 84 (2000), 3149.
- [3] GROLLIER J., CROS V., HAMZIC A., GEORGE J.M., JAFFRES H., FERT A., FAINI G., YOUSSEF J.B., LEGALL H., Appl. Phys. Lett., 78 (2001), 3663.
- [4] STILES M.D., ZANGWILL A., Phys. Rev. B, 66 (2002), 014407.
- [5] BRATAAS A., NAZAROV YU.V., BAUER G.E.W., Eur. Phys. J. B, 22 (2001), 99.
- [6] ZHANG S., LEVY P.M., FERT A., Phys. Rev. Lett., 88 (2002), 236601 (2002); SHIRO A., LEVY P.M., ZHANG S., Phys. Rev. B, 67 (2003), 104430.
- [7] BARNAS J., FERT A., GMITRA M., WEYMANN I., DUGAEV V.K., Phys. Rev. B, 72 (2005), 024426.
- [8] SUN J.Z., Phys. Rev. B, 62 (2000), 570; LI Z., ZHANG S., Phys. Rev. B, 68 (2003), 024404.
- [9] SLAVIN A.N., TIBERKEVICH V.S., Phys. Rev. B, 72 (2005), 094428.
- [10] KISELEV S.I., SANKEY J.C., KRIVOROTOV I.N., EMLEY N.C., SCHOELKOPF R.J., BUHRMAN R.A., RALPH D.C., Nature (London), 425 (2003), 380; KISELEV S.I., SANKEY J.C., KRIVOROTOV I.N., EMLEY N.C., GARCIA A.G.F., BUHRMAN R.A., RALPH D.C., Phys. Rev. B, 72 (2005), 064430.
- [11] RIPPARD W.H., PUFALL M.R., KAKA S., RUSSEK S.E., SILVA T.J., Phys. Rev. Lett., 92 (2004), 027201.
- [12] XI H., LIN Z., Phys. Rev. B, 70 (2004), 092403.

- [13] XIAO J., ZANGWILL A., STILES M.D., Phys. Rev. B, 72 (2005), 014446.
- [14] GMITRA.M., BARNAS J., Phys. Rev. Lett., 96 (2006), 207205.
- [15] RUSSEK S.E., KAKA S., RIPPARD W.H., PUFALL M.R., SILVA T.J., Phys. Rev. B, 71 (2005), 104425;
GMITRA M., BARNAS J., HORVATH D., J. Alloys. Comp., 423 (2006), 194.
- [16] BASS J., PRATT JR. W.P., J. Magn. Magn. Mater., 200 (1999), 274.

Received 7 May 2006
Revised 1 September 2006